Proceedings of the 20th National Conference on Superconductivity "New Phases, Concepts and Advances"

Dynamics of Fano-Like Resonances in Double-Quantum-Dot Systems

J. Barański[a,*] and K.J. Kapcia[b,c]

[a] *Department of General Education, Polish Air Force University, Dywizjonu 303 nr 35, 08521 Dęblin, Poland*
[b] *Institute of Spintronics and Quantum Information, Faculty of Physics, Adam Mickiewicz University in Poznań, Uniwersytetu Poznańskiego 2, 61614 Poznań, Poland*
[c] *Center for Free-Electron Laser Science CFEL, Deutsches Elektronen-Synchrotron DESY, Notkestr. 85, 22607 Hamburg, Germany*

Doi: 10.12693/APhysPolA.143.143 *e-mail: j.baranski@law.mil.pl

Quantum interference effects appearing in mesoscopic heterostructures have been extensively studied in static conditions over the last decades. It is interesting to examine the dynamics of these phenomena and get insight into the process of the formation of interference patterns. In this work, we analyze the time required for the formation of Fano-like resonances in a double quantum dot system. We examined the time evolution of conductance upon establishing an abrupt connection between quantum dots. Asymmetric Fano lines are characterized by the close coexistence of resonant enhancement and resonant suppression. Therefore, we pay particular attention to voltages, which in the static case, correspond to both these features. Our research shows that the analyzed resonances are characterized by two time scales: (i) the first one related to charge oscillations between subsystems and mostly governed by the interdot coupling constant and the relative position of energy levels of quantum dots, and (ii) the second one associated to the electron scattering on a continuum of states and responsible for the relaxation. We also show that the time required for achieving a static solution is different for voltages corresponding to local minima and local maxima.

topics: Fano-like resonance, double quantum dots, quench, time evolution

1. Introduction

The analysis of steady-state electron transport in multiple quantum dot systems proves to be valuable for understanding of the formation of quantum interference effects in various configurations. In particular, the interplay of Fano-type interference with other many-body effects such as Coulomb blockade [1, 2], Kondo resonance [3–5], or proximity-induced local pairing [6–9] were investigated both theoretically and experimentally [5, 10–13]. The analysis of electron dynamics allows for the inspection of the time required for the formation of resonances previously predicted (or observed) in stationary conditions.

Novel experimental techniques allow real-time measurements of the electron time-domain with precision below picoseconds [14–16]. Motivated by these works, we explore the time required for the formation of the Fano resonance in a T-shape double quantum dot (DQD) system (cf. Fig. 1). One of the few works considering the time evolution of Fano-like resonances in DQD systems was written by G. Michalek et. al. [17]. In their work, the authors focus mostly on the specific case when the energy level of the side dot (QD_2) coincides with the energy level of the interfacial dot (QD_1). In such a case, the abrupt coupling of a side dot causes a single Lorentzian to evolve into two peaks separated by a symmetric deep announcing destructive interference. The symmetry of the central deep is a reminiscence of the vanishing asymmetry parameter q. Traditionally, Fano-type resonance is associated with an asymmetric line shape originating from the close coexistence of resonant enhancement and resonant suppression of conductance [18]. Such a line shape in DQD conductance can be obtained when the energy level of the quasidiscrete level differs from the energy level of the main transport channel. Here, we analyze a system where the energy level of the side-attached quantum dot is slightly shifted from the energy level of the interfacial dot. This approach allows for the inspection of the evolution of both the resonant peak and the deep in their recognizable shape.

2. Investigated system

The setup discussed in this work is schematically presented in Fig. 1 and it is composed of two quantum dots hybridized with two metallic electrodes. In this configuration, we assume that one of QDs is

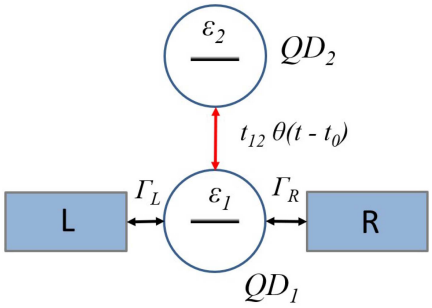

Fig. 1. Scheme of the considered system consisting of two quantum dots (QD_1 and QD_2) and two external electrodes (L and R) connected in a T-shape geometry. Here, Γ_L and Γ_R denote the coupling strengths of QD_1 to the electrodes, while the time-dependent $t_{12}\theta(t-t_0)$ represents the interdot coupling.

strongly hybridized to the external electrodes, while the second one is coupled only to the first QD. In such a configuration, the interference of electrons transmitted between the source and drain electrode via the interfacial quantum dot (QD_1) and electrons scattered on the side level of QD_2 give rise to Fano-like interference. Fingerprints of such interferences can be observed as asymmetric lines in differential conductance [11]. In this work, we will estimate how much time it takes for such interference patterns to emerge upon a sudden connection between the dots or, equivalently, a sudden switch of the energy level of the side dot.

The considered system can be described in terms of the Anderson-like Hamiltonian which reads as

$$\hat{H} = \sum_{\beta=L,R} (\hat{H}_\beta + \hat{H}_{T\beta}) + \sum_{i=1,2} \hat{H}_{QDi} + \hat{H}_t, \quad (1)$$

where $\hat{H}_\beta = \sum_{k,\beta,\sigma} \xi_{k\beta} \hat{c}^\dagger_{k\beta\sigma} \hat{c}_{k\beta\sigma}$ corresponds to the external electrodes $\beta = L, R$ treated as a free electron gas, where the electron energies $\xi_{k\beta}$ are measured with respect to the corresponding chemical potentials μ_β. The chemical potentials are tunned when the voltage V is applied across the junction, i.e., $\mu_L - \mu_R = eV$. Two single-level non-correlated quantum dots Hamiltonian and the tunnel coupling between them are represented by, respectively, $\hat{H}_{QDi} = \sum_\sigma \epsilon_i \hat{d}^\dagger_{i\sigma} \hat{d}_{i\sigma}$ and $\hat{H}_t = \sum_\sigma \theta(t-t_0)\, t_{12}\, (\hat{d}^\dagger_{1\sigma} \hat{d}_{2\sigma} + \hat{d}^\dagger_{2\sigma} \hat{d}_{1\sigma})$, where t_0 represents the time at which the side dot (QD_2) is abruptly coupled to interfacial one (QD_1) with a interdot hoping strength t_{12}, and $\theta(t)$ is the Heaviside step function. It is useful to introduce the reduced time parameter $\tilde{t} = t - t_0$, which represents the time elapsed from the quench. The term $\hat{H}_{T\beta} = \sum_{k,\sigma} V_{k\beta\sigma} (\hat{c}_{k\beta\sigma} \hat{d}^\dagger_{1\sigma} + \text{h.c.})$ stands for hybridization of each electrode to an interfacial quantum dot. We introduce the wide-band limit coupling constant $\Gamma_\beta = \pi \sum_{k,\sigma} |V_{k\beta\sigma}|^2 \delta(\omega - \xi_{k\beta})$. In our calculations, the total coupling of QD_1 to the external electrodes $\Gamma_N = \Gamma_L + \Gamma_R$ is used as the energy unit, i.e., $\Gamma_N \equiv 1$ (we assume $V_{kL\sigma} = V_{kR\sigma}$ and $\Gamma_L = \Gamma_R$).

Our aim is to calculate the time-dependent differential conductance $G(t, eV) = \frac{\mathrm{d}I}{\mathrm{d}V}$. We adopt a method that was used previously in [19]. The charge current $I(t)$ (assuming $e = h \equiv 1$) can be calculated using the following equation

$$I(t) = 2\,\mathrm{Im}\left\{ \sum_{k,\sigma} \left[V_{kL\sigma} \langle \hat{d}^\dagger_{1\sigma}(t) \hat{c}_{kL\sigma}(0) \rangle - \frac{\mathrm{i}\,\Gamma_L \langle \hat{n}_{1\sigma}(t) \rangle}{2} \right] \right\} \quad (2)$$

and it is encoded in two time-dependent averages: (i) QD_1 occupation number $n_{1\sigma}(t) = \langle \hat{d}^\dagger_{1\sigma}(t) \hat{d}_{1\sigma}(t) \rangle$ and (ii) dot-lead correlation function $\langle \hat{d}^\dagger_{1\sigma}(t) \hat{c}_{kL\sigma}(0) \rangle$. In our approach, we calculate a set of ordinary differential equations of motion for the desired averages in the Heisenberg representation, and use the fourth-order Runge–Kutta method to solve these equations numerically. We assume the following initial conditions: $n_{1\uparrow}(0) = n_{1\downarrow}(0) = 1$ and $n_{2\uparrow}(0) = n_{2\downarrow}(0) = 0$ ($n_{i\sigma} = \langle \hat{n}_{i\sigma} \rangle = \langle \hat{d}^\dagger_{i\sigma} \hat{d}_{i\sigma} \rangle$).

The quench protocol. In order to minimize the influence of dot-lead coupling on transient effects, i.e., conductance oscillations, the quench protocol assumes that at first (at $t = 0$) only QD_1 is coupled to the external electrodes and we wait long enough for a well-pronounced central peak emerging around $eV \sim \epsilon_1$ with all fluctuations suppressed (cf. [20]). After t_0 (where t_0 is much larger than the time required for thermalization), the side dot is abruptly connected and we observe the evolution of the Fano resonance near ϵ_2. In particular, we will focus on the evolution of conductance for the source-drain (S-D) voltages corresponding to the position of resonant enhancement and resonant suppression (obtained in static conditions).

3. Time-evolution of conductance

The resonances analyzed in this work are characterized by two time scales. One of them is related to charge oscillations between subsystems and is mostly governed by the interdot coupling constant t_{12} and the relative position of the energy levels $\epsilon_1 - \epsilon_2$. Another one is associated with electron scattering on the continuum of states, which is responsible for relaxation and which is governed by Γ_N. The total time of achieving stationary conditions results from these two processes.

To gain an overall view of conductance evolution, we present a density plot (Fig. 2) that shows the differential conductance as a function of source-drain voltage and time, obtained for $\epsilon_1 = 0$ and $\epsilon_2 = \Gamma_N$. Initially (at time $t = 0$) QD_1 is coupled only to electrodes L and R. Around $\epsilon_1 = 0$, we can observe the evolution of the Lorentz curve and small fluctuations on side of it. After a few units of time

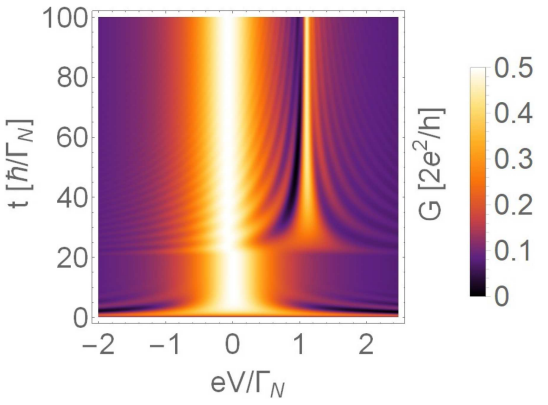

Fig. 2. Density plot of differential conductance as a function of source-drain voltage (eV) and time (t) obtained for $t_{12} = 0.3\Gamma_N$ ($\epsilon_1 = 0$, $\epsilon_2 = \Gamma_N$).

(being $\hbar/\Gamma_N$) the fluctuations are suppressed and the Lorentz curve centered at ϵ_1 achieves its stable shape. Safely later, at $t_0 = 20\hbar/\Gamma_N$, we abruptly connect the second quantum dot. In the vicinity of ϵ_2, a resonant enhancement is visible and resonant depletion of conductance starts to evolve. One could note strong conductance oscillations on both sides of these features. The frequency of the oscillations is the higher, the farther eV is from the resonant feature. One can note that those fluctuations are tuned down by a similar factor after each cycle. Consequently, the relaxation process of the oscillations is the faster, the farther they are from the resonant feature. In Fig. 2 one can see that oscillations near the resonant feature are still pronounced well even after $t = 100\hbar/\Gamma_N$, while oscillations far away from the feature (e.g., at $eV = -\Gamma_N$) are strongly reduced at $t \simeq 40\hbar/\Gamma_N$.

However, in very close vicinity of ϵ_2, resonant enhancement appears and increases monotonically without oscillations. The evolution of the resonant minima (which in the static case appears exactly at $eV = \epsilon_2$) resembles damped oscillations. According to [17], the oscillations of transmittance for $\epsilon_1 = \epsilon_2 \equiv \epsilon$ in the very weak coupling regime $t_{12} \ll \Gamma_N$ are dependent on the difference between S-D voltage and the energies of quantum dots ($eV - \epsilon$). In such conditions, the transmittance (and conductance) for energy (voltage) corresponding to local minima, i.e., $\omega = \epsilon$ ($eV = \epsilon$) after quench is continuously tuned down without oscillations. Our results indicate that for $\epsilon_2 \neq \epsilon_1$, conductance oscillations have vanishing frequency not for eV corresponding to local minima (ϵ_2), but for nearby local maxima.

In the static conditions, the energy corresponding to local maxima is given by $f_r = \frac{1}{2}\big(\epsilon_1+\epsilon_2 \pm \sqrt{(\epsilon_1-\epsilon_2)^2 + 4t_{12}^2}\big)$, where the sign "+" refers to the case when $\epsilon_2 > \epsilon_1$ and "−" to the opposite case. Note that for a vanishing interdot coupling $t_{12} \to 0^+$, one gets $f_r \to \epsilon_2 \pm 0^+$. Indeed, for a very weak t_{12}, the resonant enhancement and resonant suppression occur in very close vicinity. The Fano minima appear exactly at $eV = \epsilon_2$ (at the static conditions), thus for the nonvanishing t_{12}, it is slightly shifted from $eV = f_r$, which explains why conductance as a function of time under these conditions resembles damped oscillations.

TABLE I

Local extrema relaxation times $\tau_{\min}$ and $\tau_{\max}$ obtained for $\epsilon_1 = 0$, $\epsilon_2 = \Gamma_N$, and several couplings t_{12}.

t_{12} [Γ_N]	$\tau_{\min}$ [$\hbar/\Gamma_N$]	$\tau_{\max}$ [$\hbar/\Gamma_N$]
0.3	40.70	16.85
0.4	19.78	10.37
0.5	12.53	7.42
0.6	9.06	5.89

TABLE II

Local extrema relaxation times $\tau_{\min}$ and $\tau_{\max}$ obtained for $\epsilon_1 = 0$, $t_{12} = 0.5\Gamma_N$, and several energies ϵ_2.

ϵ_2 [Γ_N]	$\tau_{\min}$ [$\hbar/\Gamma_N$]	$\tau_{\max}$ [$\hbar/\Gamma_N$]
0.0	2.76	2.44
0.25	3.41	2.93
0.5	5.67	3.69
1.0	12.53	7.42
1.5	19.07	9.71

3.1. Relaxation time

In order to quantify the relaxation process, we fit an exponential function representing the decay of the difference between the initial and the final value of conductance at voltages corresponding to local minima (i.e., $eV = \epsilon_2$) and local maxima (i.e., $eV = f_r$). Such a function can be read as

$$G(t - t_0) = G(\infty) - \Big[G(\infty) - G(t_0)\Big] \exp\left(\frac{t_0 - t}{\tau}\right), \tag{3}$$

where $G(t_0)$ and $G(\infty)$ represent the conductance values, respectively, just after the quench and in the static conditions. The relaxation factor τ represents the time after which the difference between the initial and final value of conductance decreases $e \simeq 2.718$ times. Determined values of $\tau_{\min}$ and $\tau_{\max}$ corresponding to the found time evolution of the investigated features in the static local minima and maxima, respectively, for $\epsilon_2 = \Gamma_N$ and $\epsilon_1 = 0$ and several values of t_{12} are presented in Table I. The fitting of function (3) was performed to the data presented in Figs. 3 and 4. Analogously, the results for the fixed constant coupling $t_{12} = 0.5\Gamma_N$ and a few energies of the side dot ϵ_2 are presented in Table II (cf. also Fig. 5).

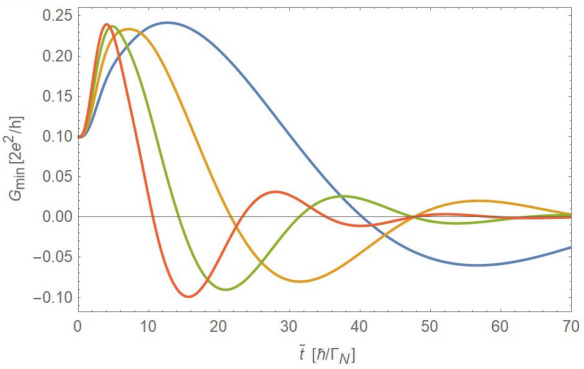

Fig. 3. Suppression of conductance at static minima (i.e., for $eV = \epsilon_2$) obtained for $t_{12} = 0.3\Gamma_N$ (blue line), $t_{12} = 0.4\Gamma_N$ (orange line), $t_{12} = 0.5\Gamma_N$ (green line), $t_{12} = 0.6\Gamma_N$ (red line); cf. also Fig. 4 for corresponding colour legend ($\epsilon_1 = 0$, $\epsilon_2 = \Gamma_N$).

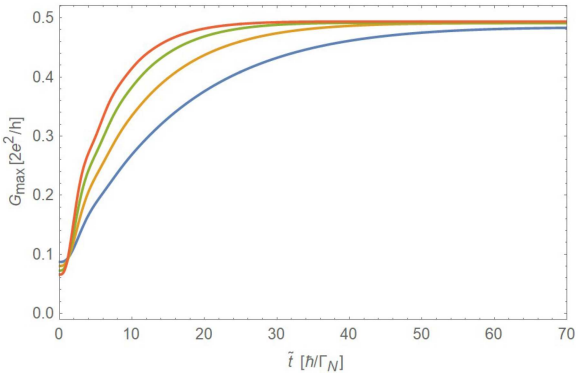

Fig. 4. Evolution of the resonant enhancement of conductance calculated at a voltage corresponding to static maxima (i.e., for $eV = f_r$) obtained for $t_{12} = 0.3\Gamma_N$ (blue line), $t_{12} = 0.4\Gamma_N$ (orange line), $t_{12} = 0.5\Gamma_N$ (green line), $t_{12} = 0.6\Gamma_N$ (red line); corresponding colour lines are given from the bottom-right ($\epsilon_1 = 0$, $\epsilon_2 = \Gamma_N$).

From both tables one can notice that the difference in the obtained relaxation times for local maxima and minima is greater for smaller interdot couplings. On the contrary, the smallest difference of relaxation times occurs when ϵ_2 coincides with ϵ_1 and interdot coupling is strong.

3.2. Extrema evolution

Damped oscillations near static minima (briefly discussed in the previous section) for different couplings t_{12} are presented in Fig. 3. Analyzing Figs. 2 and 3, one can note that the amplitude of the oscillations diminishes by a similar factor after each full period (independently of t_{12}). The period of such oscillations, however, is dependent on t_{12} and the relative position of the initial energy levels ($\epsilon_1 - \epsilon_2$) (cf. Fig. 5). In the case of weak interdot coupling, the period is considerably larger and the stationary condition is achieved much later. Analyzing the

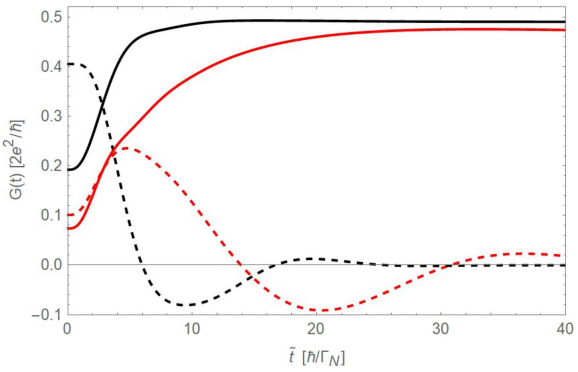

Fig. 5. Comparision of minima (dashed lines, located at $eV = \epsilon_2$) and maxima (solid lines, located at $eV = f_r$) evolution obtained for $\epsilon_2 = 0.25\Gamma_N$ (black lines) and $\epsilon_2 = \Gamma_N$ (red lines). The other parameters are taken as $\epsilon_1 = 0$ and $t_{12} = 0.5\Gamma_N$.

evolution of the structure near $eV \simeq f_r$, we notice that the enhancement of conductance is monotonic over time (oscillations are not present). In Figs. 3 and 4, we see that the monotonic building up of the resonant peak is considerably faster than the resonant suppression (cf. also Table I). To emphasize this observation one can, e.g., compare the values of each feature near $\tilde{t} \simeq 50\hbar/\Gamma_N$. The values of the maxima for all values of t_{12} studied (except for $t_{12} = 0.3$) are very close to stable, while for the minima one can still see clear oscillations for all t_{12}.

The relative position of energy levels of the quantum dots (i.e., $\epsilon_1 - \epsilon_2$) has the opposite effect on the period and the relaxation process than t_{12}. Namely, the time required to achieve stationary conditions is longer when ϵ_2 is shifted far away from ϵ_1. This can be seen in Fig. 5 and Table II collecting estimated relaxation times for a few different ϵ_2.

4. Conclusions

In this work, we investigated the dynamics of the Fano resonance in a double quantum dot system. The time dependence of conductance versus source-drain voltages and the evolution of local minima and maxima after the quench are presented. conductance oscillations for voltages corresponding to a static position of the local minima were obtained. The period of these oscillations and the relaxation time depend on both the coupling t_{12} between the dots and the relative position $\epsilon_1 - \epsilon_2$ of dots energies. On the other hand, for voltages corresponding to the maxima, frequency of oscillations tends to 0 and, consequently, building up of the resonant enhancement occurs in monotonic way. We calculated the characteristic times for relaxation processes $\tau_{\min}$ and $\tau_{\max}$ for the local minima and the local maxima. We found that difference between these times strongly depends on t_{12} and $\epsilon_1 - \epsilon_2$. However, for

all ranges of considered parameters, the formation of the resonant enhancement is faster than the resonant depletion of conductance.

Acknowledgments

We thank Magdalena Barańska for very fruitful discussions. K.J.K. thanks the Polish National Agency for Academic Exchange for funding in the frame of the Bekker programme (PPN/BEK/2020/1/00184).

K.J.K. is also grateful for the funding from the scholarships of the Minister of Science and Higher Education (Poland) for outstanding young scientists (2019 edition, No. 821/STYP/14/2019). The equations of motion in the Heisenberg representation have been derived using SNEG library created by R. Žitko [21].

References

[1] H. Lu, R. Lü, B. fen Zhu, *Physica E* **34**, 538 (2006).

[2] A.C. Johnson, C.M. Marcus, M.P. Hanson, A.C. Gossard, *Phys. Rev. Lett.* **93**, 106803 (2004).

[3] B.R. Bułka, P. Stefański, *Phys. Rev. Lett.* **86**, 5128 (2001).

[4] R. Žitko, *Phys. Rev. B* **81**, 115316 (2010).

[5] S. Sasaki, H. Tamura, T. Akazaki, T. Fujisawa, *Phys. Rev. Lett.* **103**, 266806 (2009).

[6] A.M. Calle, M. Pacheco, G.B. Martins, V.M. Apel, G.A. Lara, P.A. Orellana, *J. Phys. Condens. Matter* **29**, 135301 (2017).

[7] J. Barański, T. Zienkiewicz, M. Barańska, K.J. Kapcia, *Sci. Rep.* **10**, 2881 (2020).

[8] J. Barański, T. Domański, *Acta Phys. Pol. A* **121**, 1213 (2012).

[9] J. Barański, T. Domański, *Phys. Rev. B* **84**, 195424 (2011).

[10] K. Kobayashi, H. Aikawa, S. Katsumoto, Y. Iye, *Phys. Rev. B* **68**, 235304 (2003).

[11] K. Kobayashi, H. Aikawa, S. Katsumoto, Y. Iye, *Phys. Rev. Lett.* **88**, 256806 (2002).

[12] M. Sato, H. Aikawa, K. Kobayashi, S. Katsumoto, Y. Iye, *Phys. Rev. Lett.* **95**, 066801 (2005).

[13] K. Kobayashi, H. Aikawa, A. Sano, S. Katsumoto, Y. Iye, *Phys. Rev. B* **70**, 035319 (2004).

[14] A.L. Cavalieri, N. Müller, T. Uphues et al., *Nature* **449**, 1029 (2007).

[15] M. Hentschel, R. Kienberger, C. Spielmann, G.A. Reider, N. Milosevic, T. Brabec, P. Corkum, U. Heinzmann, M. Drescher, F. Krausz, *Nature* **414**, 509 (2001).

[16] R. Kienberger, E. Goulielmakis, M. Uiberacker et al., *Nature* **427**, 817 (2004).

[17] G. Michałek, B.R. Bułka, *J. Magn. Magn. Mater.* **544**, 168700 (2022).

[18] U. Fano, *Phys. Rev.* **124**, 1866 (1961).

[19] J. Barański, M. Barańska, T. Zienkiewicz, R. Taranko, T. Domański, *Phys. Rev. B* **103**, 235416 (2021).

[20] J. Barański, M. Barańska, T. Zienkiewicz, K.J. Kapcia, arXiv:2207.14022 2022.

[21] R. Žitko, *Comput. Phys. Commun.* **182**, 2259 (2011).